Comparison of laboratory calibrations of the Airborne Visible/Infrared Imaging Spectrometer (AVIRIS) at the beginning and end of the first flight season

Gregg Vane, Thomas G. Chrien, John H. Reimer, Robert O. Green, and James E. Conel

Jet Propulsion Laboratory, California Institute of Technology
4800 Oak Grove Drive, Pasadena, California 91109

ABSTRACT

Spectral and radiometric calibrations of the Airborne Visible/Infrared Imaging Spectrometer (AVIRIS) were performed in the laboratory in June and November, 1987, at the beginning and end of the first flight season. This paper describes those calibrations and the changes in instrument characteristics that occurred during the flight season as a result of factors such as detachment of the optical fibers to two of the four AVIRIS spectrometers, degradation in the optical alignment of the spectrometers due to thermally-induced and mechanical warpage, and breakage of a thermal blocking filter in one of the spectrometers. These factors caused loss of signal in three spectrometers, loss of spectral resolution in two spectrometers, and added uncertainty in the radiometry of AVIRIS. Results from in-flight assessment of the laboratory calibrations are presented. The paper concludes with a discussion of improvements made to the instrument since the end of the first flight season and plans for the future. Improvements include (1) a new thermal control system for stabilizing spectrometer temperatures, (2) kinematic mounting of the spectrometers to the instrument rack, and (3) new epoxy for attaching the optical fibers inside their mounting tubes.

1. INTRODUCTION

AVIRIS is a second-generation imaging spectrometer developed at the Jet Propulsion Laboratory (JPL) for use in earth remote sensing studies across a broad spectrum of scientific disciplines, including botany, geology, hydrology, oceanography, and atmospheric science.[1] Design and construction of the sensor and ground data processing facility were begun in 1984 and completed in June 1987. Following a laboratory calibration, flight operations were begun on June 25, 1987. Data were collected for 20 investigators between June and October 1987, after which the instrument was returned to JPL for a post-flight-season calibration and refurbishment. In this paper, we give a synopsis of the procedures used in the laboratory spectral and radiometric calibration of AVIRIS, and show results obtained from the two laboratory calibrations conducted in 1987 and from flight experiments also conducted in 1987 to assess the performance of the instrument. As background, a brief description of the instrument follows. Complete details of the sensor and ground data processing system can be found in Volume 834 of the Proceedings of the SPIE.[2-8]

AVIRIS acquires images in 220 contiguous 10-nanometer (nm) spectral bands in the region between 0.40 and 2.45 micrometers (μm). The instantaneous field of view of AVIRIS is 1 milliradian and the field of view as defined by the scan angle is 30 degrees. This results in images covering a 10.5 km swath composed of picture elements (pixels) that subtend 20 m on the ground from the 20 km altitude of the NASA U-2 and ER-2 aircraft. AVIRIS gathers spectral images in the whisk-broom imaging mode, employing foreoptics with a mirror that scans in one direction, then rapidly returns to the start position for the next scan line. A diagram of the optical configuration is shown in Figure 1. An artist's rendition of the flight hardware is shown in Figure 2. The scan rate and detector readout timing were designed to provide a 17 percent spatial oversampling at sea level in both the cross-track and along-track dimensions in order to assure complete spatial coverage over mountainous terrain. This results in the acquisition of 614 pixels in each scan line. Geometric rectification removes the oversampling, resulting in an image 550 pixels across. Twelve scans are completed per second. During the fly-back portion of each scan cycle, a shutter closes the foreoptics from the rest of the optical system, and a single measurement of the detector dark current for each of the detector elements is recorded.

The foreoptics are connected to four spectrometers with optical fibers (see Figure 1). Spectrometer A contains a 32-element line array of silicon detectors, and spectrometers B, C, and D each employ 64-element line arrays of indium antimonide detectors. While a total of 224 spectral bands are actually acquired, the readout architecture of the detector arrays renders the first band of each array unusable; there are thus 220 usable raw spectral bands. The effective spectral ranges of spectrometers A, B, C, and D are 0.40 to 0.71, 0.68 to 1.28, 1.24 to 1.86, and 1.83 to 2.45 μm, respectively, as aligned for the 1987 flight season. There is an overlap of 3 to 4 spectral bands in coverage of the spectrum between the 4 spectrometers. During radiometric calibration the spectral region covered by the 220 raw spectral bands can, at the request of the investigator, be resampled to remove overlap between spectrometers and equalize the spectral sampling interval across the entire 0.40 to 2.45 μm region. This resampling results in 210 spectral bands over the 0.40 to 2.45 μm region.

Each spectrometer additionally receives input via a second optical fiber from an onboard radiometric and spectral calibration source consisting of a tungsten lamp, a four-position filter wheel containing two neutral density filters, a didymium oxide filter and an opaque position.[2] The neutral density filters provide broad-spectral-band energy at two intensity levels to monitor radiometric stability. The didymium oxide filter provides several spectral absorption features in each of the spectral regions of the four AVIRIS spectrometers to monitor wavelength calibration. The opaque position is used in conjunction with the shutter in the foreoptics to provide a measurement of dark current from each detector. In each of the 4 filter positions, a full scan line of data (614 readouts of the detectors) is acquired.

In the following section of the paper we describe the procedures used in the laboratory to perform spectral and radiometric calibrations of AVIRIS. A summary of the calibration accuracies achieved in the pre-flight-season lab calibration is also given. Following that is a comparison of the pre- and post-flight-season calibrations and an in-flight assessment of instrument performance. Instrument factors that caused a degradation in performance over the course of the flight season are also discussed. We conclude with a discussion of improvements that have been made to AVIRIS over the past winter and spring, and plans for the future.

2. LABORATORY CALIBRATION OF AVIRIS

AVIRIS calibration is broken into two major parts, spectral and radiometric. Each requires its own support equipment and procedures, and each has associated with it an error budget that defines the accuracies achieved. The following discussion is a summary of a more detailed discussion found in Reference 9.

SPIE Vol. 924 pp. 168-178 Recent Advances in Sensors, Radiometry, and Data Processing for Remote Sensing (1988)

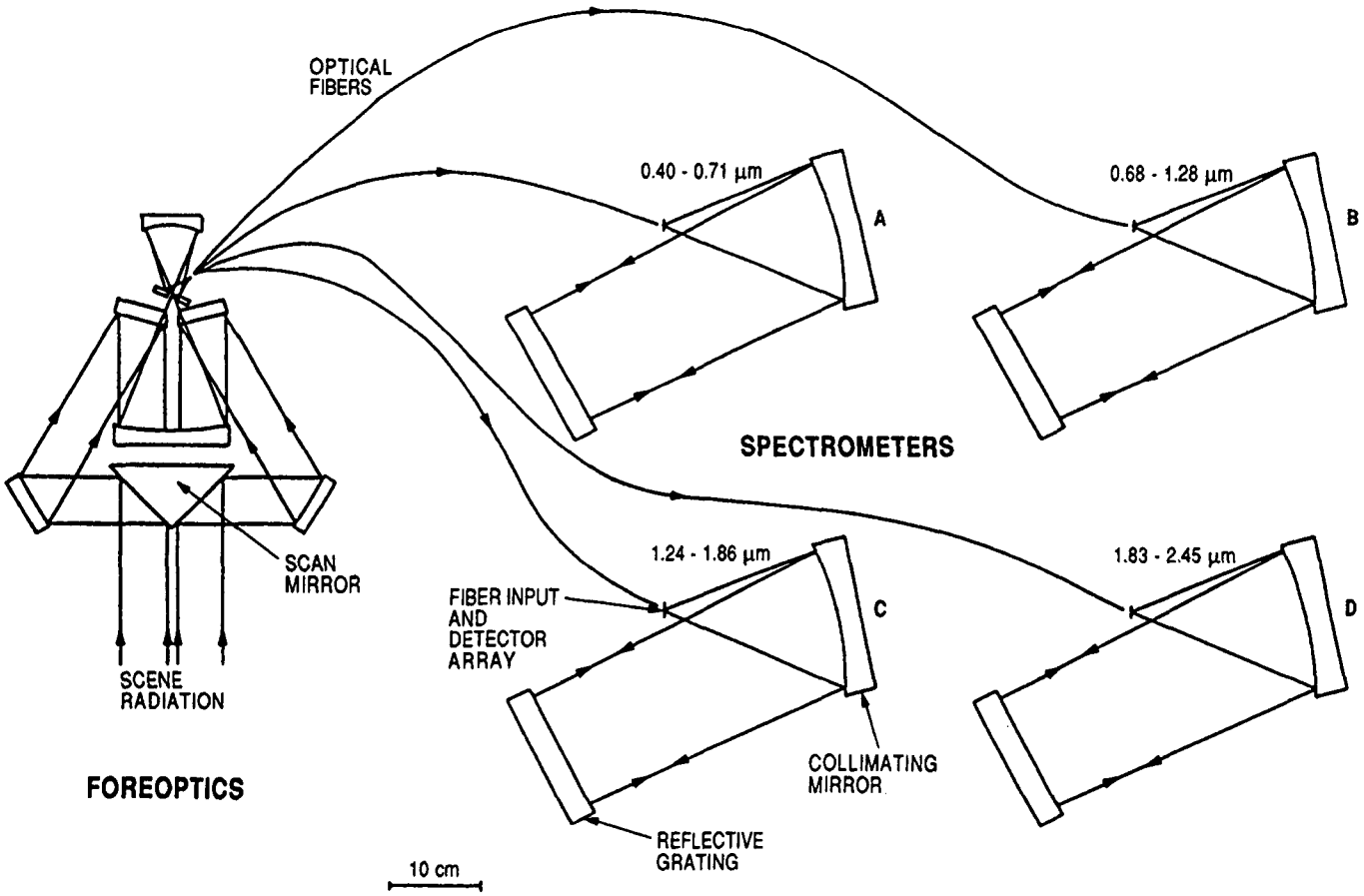

Figure 1. Schematic diagram of the AVIRIS optical configuration. The scanning foreoptics on the right are connected to the four spectrometers on the left with optical fibers.[26]

2.1. Spectral calibration

The three goals that must be met in the spectral calibration of an imaging spectrometer are: (1) Mapping of the center wavelength of light falling on each detector element, (2) determination of the wavelength bandwidth falling on each detector element, and (3) determination of the spectral sampling interval of each spectrometer. The purpose of the spectral calibration of AVIRIS is to determine the normalized instrument response function. This function is closely approximated by a Gaussian curve that is completely characterized by the wavelength of maximum response and by the spectral width at half peak height (the so-called full width at half maximum, FWHM). The distance between the maxima of the response functions of adjacent detectors is the spectral sampling interval. The optical setup for performing the spectral calibration is shown schematically in Figure 3. A Jarrell-Ash model 82-487 monochromator and tungsten lamp are used in the calibration. The monochromator is calibrated with a mercury pen lamp using multiple orders of the emission line at 546.1 nm. Three different gratings are used alternately in the monochromator to cover the full spectral range of AVIRIS. The monochromator is calibrated each time a grating change is made. By choosing the widths of the entrance and exit slits of the monochromator, the bandwidth of the exiting light can be tailored as required; typically, a bandwidth of 1 nm is used. The output signal level from a given AVIRIS detector element is recorded as the wavelength output of the monochromator is scanned in steps of 1 nm. This is plotted against the input wavelength as determined from the monochromator calibration, to produce a spectral response curve as shown in Figure 4. Analysis of the spectral response consists of fitting a Gaussian curve to the normalized signal using as the fit parameters the wavelength of maximum response and the FWHM spectral bandwidth. This procedure is followed for several detector elements per spectrometer. A linear fit is applied to the wavelengths of maximum response as a function of detector element number to determine the center wavelength positions of the other detector elements in a given spectrometer for which spectral response curves are not acquired. From the center wavelength positions of the 224 detector elements, the spectral sampling interval is determined. This is also the slope of the line fit to the wavelengths of the maximum response for each spectrometer. The results from the pre-flight-season spectral calibration of AVIRIS are summarized in Table 1.

2.2. Radiometric calibration

The goals of radiometric calibration are to establish and apply a set of calibration multipliers which: (1) Convert AVIRIS output digital numbers (DNs) to radiance ($\mu W/cm^2$-sr-nm) accurate to at least 10 percent absolute, and (2) to correct for non-uniformity in the response of the AVIRIS detector elements to at least 0.5 percent. Achieving these goals requires four major steps: (1) Calibration of a spectro-

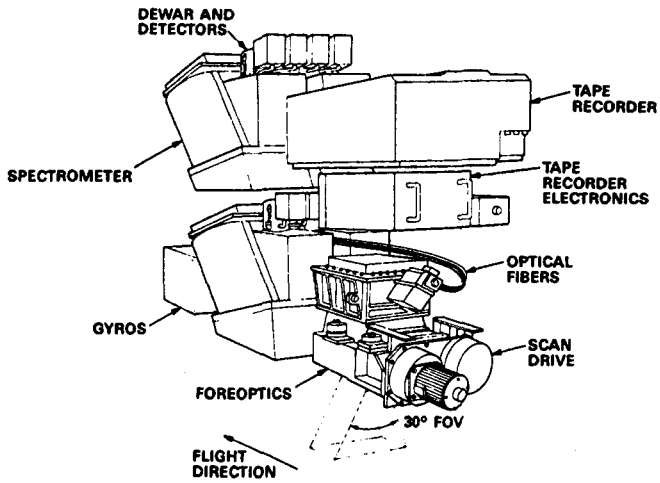

Figure 2. Artist's drawing of the AVIRIS flight hardware showing the physical layout of the major subsystems. The various electronics subassemblies are omitted for clarity.[26]

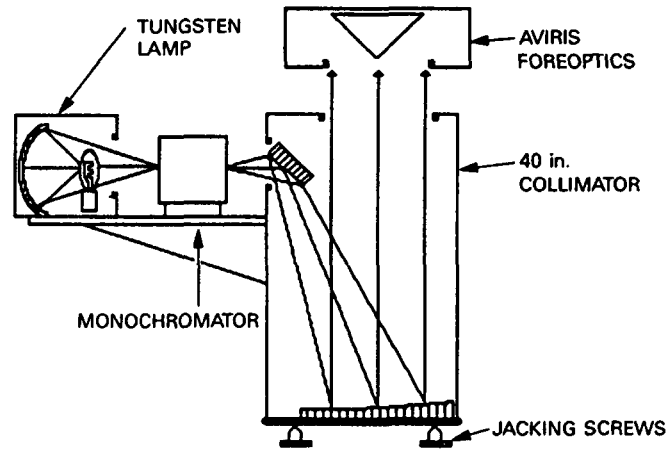

Figure 3. Laboratory setup used in performing the spectral calibration of AVIRIS.[9]

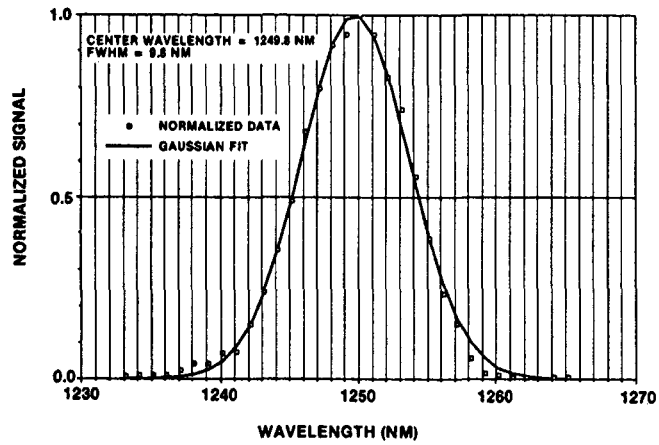

Figure 4. A typical normalized AVIRIS spectral response function for channel 98, Spectrometer C.

Table 1. AVIRIS 1987 Pre-Flight-Season Spectral Calibration[9]

PARAMETER (IN UNITS OF NM)	SPECTROMETER A	B	C	D
AVERAGE BANDWIDTH (FWHM)	9.7	9.7	9.0	11.6
SPECTRAL SAMPLING INTERVAL	10.0	9.58	9.86	9.85
STD. DEV. OF LINEARITY MEASUREMENT	0.71	0.60	0.58	1.84
MONOCHROMATOR CALIBRATION UNCERTAINTY	0.5	0.5	0.5	1.0
AVIRIS SPECTRAL CALIBRATION ACCURACY	0.9	0.8	0.8	2.1

radiometer against a National Bureau of Standards (NBS) traceable lamp, (2) calibration of an integrating sphere with the calibrated spectroradiometer, (3) acquisition of a file of AVIRIS DNs while viewing the calibrated integrating sphere, and (4) calculation of a table of multipliers tying the AVIRIS DN to the integrating sphere output radiance.

The laboratory setup used in calibrating the spectroradiometer and integrating sphere is shown in Figure 5. An Optronics Laboratories model 746 spectroradiometer is placed on a rotating stage to view alternately a freshly prepared pressed halon target at a 45 degree angle normal to its surface, and a Labsphere, Inc., 40 inch diameter integrating sphere. The halon target is illuminated with a tungsten lamp calibrated as a standard of irradiance by Optronics Laboratories against an NBS-calibrated lamp. The irradiance standard is powered by an Optronics calibrated constant-current power supply. A file of spectral radiance values for the standard lamp-halon target-spectroradiometer configuration in Figure 5 is calculated using the expression

$$L(\lambda) = E(\lambda)\, R(\lambda)\, (50\ \text{cm})^2 / \pi\, (D\ \text{cm})^2 \qquad (1)$$

where $L(\lambda)$ is the radiance viewed by the spectroradiometer, $E(\lambda)$ is the irradiance of the calibrated lamp provided by the manufacturer, $R(\lambda)$ is the reflectance of the halon target,[10] 50 cm is the distance at which the lamp was calibrated, and D is the distance between the lamp and the halon target in the setup in Figure 5. This file is used subsequently to convert spectroradiometer output DN to radiance when calibrating the Labsphere, Inc., integrating sphere.

In an earlier paper[9], there was incorrectly included a cos 45 term in the numerator of the right hand side of the above equation; this term was correct for an earlier calibration setup in which the halon target was 45 degrees to the calibrated lamp and normal to the spectroradiometer. In the configuration shown in Figure 5 and used in calibrating the spectroradiometer for AVIRIS calibrations, the cos 45 term does not apply.

After the spectroradiometer has been calibrated, it is rotated to a position for viewing the 16 inch output port of the integrating sphere. After a 30 minute warmup period, data are acquired from the integrating sphere at several output levels. The intensity of the integrating sphere output is controlled by changing fixed apertures located between the tungsten lamps and the interior of the sphere. The uniformity of output across the 16 inch output port was measured and found to be uniform to within 1% across the port for those aperture settings used in calibrating AVIRIS. Calibration of successive integrating sphere output levels is alternated with repeated calibration of the spectroradiometer. The radiance output of the integrating sphere has been measured to be constant to within 1.1% over a typical calibration period.

To calibrate AVIRIS, the integrating sphere is positioned so that the plane of the output port of the sphere is 12 inches beneath the AVIRIS foreoptics. The same baffles are used in this setup as shown in Figure 5. The U-2 hatch window, a 16-inch-diameter, 1-inch-thick piece of water-free quartz, is positioned above the integrating sphere output port at the same distance from the AVIRIS foreoptics as in the aircraft. Twenty consecutive sets of data are recorded by AVIRIS from two integrating sphere output levels chosen to provide adequate light levels across the full AVIRIS spectral region. Linearity of response of AVIRIS was confirmed by viewing the integrating sphere at 12 output intensities; thus, a single output level in combination with the zero point on the radiance versus DN plot is adequate for constructing the calibration file. In practice, the highest output level (AAAA, in the integrating sphere nomenclature) and the zero point on the radiance/DN curve are used to calibrate the first half of the spectral range of spectrometer A, while a lower output level (EEEE) and the zero point are used for the remainder of the AVIRIS spectral range.

The calibration file used to convert AVIRIS DN values into radiance values is a set of multipliers consisting of 32-bit real numbers generated from the laboratory calibration data. These data consist of two components: radiance measurements of the two integrating sphere intensity levels taken with the spectroradiometer, and data taken with AVIRIS while viewing the integrating sphere at the same two intensity levels. The first step in generating the calibration file is subtraction of the dark current from the AVIRIS data. The next step is to associate the 614 cross-track mean DN values of every spectral band with the corresponding radiance value for that spectral band, computed by resampling the spectroradiometer measurements to match the spectral spacing of the AVIRIS detector elements. The final set of multipliers, M(s,b), is computed as follows:

$$M(s,b) = L(b) / DN(s,b) \qquad (2)$$

where s is the cross-track sample number, b is the spectral band number, L(b) is the radiance of the integrating sphere, and DN(s,b) is the signal level recorded by AVIRIS. This set of 224 x 614 multipliers is saved as the calibration file and used in the radiometric calibration of all subsequent AVIRIS data.

The radiometric calibration of AVIRIS flight data converts 10-bit DN values to 32-bit real-number radiance values in units of $\mu W/cm^2$-nm-sr and linearly scales the values to 16-bit integers. In the process, dark current subtraction, detector equalization, resampling to account for detector readout delays, and, optionally, reconstruction of the full spectrum accounting for spectral band overlap and varying spectral spacings between spectrometers are performed. One dark current value for each detector element is recorded at the end of each scan line. Dark current subtraction is done using a sliding mean of 101 dark current values such that the dark current correction for a given scan line is the mean of the dark current recorded at the end of that scan line and the dark current values recorded at the ends of the 50 scan lines before and after that scan line. The next step is detector response compensation, which corrects for the non-uniformity of responses of the 224 detector elements. Using the multipliers stored in the calibration file, DN values are converted to 32-bit radiance values. Application of the multipliers at this point also removes the cross-track response asymmetry caused by foreoptics vignetting. Resampling to correct for detector readout delays is performed next. These delays occur because the detector elements in the line arrays are read sequentially. This results in the last element of an array acquiring a signal from a spot on the ground approximately one pixel further across the scan than that acquired by the first element. Linear interpolation is performed between successive pixels within a scan line. Following this, the full spectrum is reconstructed. Resampling is performed in the spectral direction to correct for spectral band overlap between spectrometers and to create a spectrum with uniform spacing of spectral band center wavelengths. The first detector element in each spectrometer is bypassed during the interpolation for reasons discussed earlier. (The spectral resampling in this step in radiometric correction processing was performed routinely on all data processed from the first flight season; it is now being offered as an option for the benefit of those investigators wishing un-resampled data.) The spectral resampling step produces 210 spectral bands from 0.4000 to 2.4482 μm with 9.8 nm spectral sampling. Finally, the 32-bit real-number radiance values are converted to 16-bit integers by multiplying each radiance value by a factor of 100 and rounding to the nearest integer value.

The error budget for the AVIRIS pre-flight-season laboratory radiometric calibration is summarized in Table 2. Details of the error analysis are given in Reference 9. Briefly, the integrating sphere calibration accuracy was determined through a propagation-of-errors analysis[11] of measured and estimated uncertainties associated with the calibration of the spectroradiometer and integrating sphere; the thermally induced drift in AVIRIS signal output was measured in the lab through repeated calibrations over time; the vibrationally induced output drifts were determined from the same data; the polarization sensitivity represents the worst case scenario of 100% polarization, which does not occur on the earth's surface, and was measured using visible and infrared polarizing filters; the radiometric effect of uncertainty in the spectral calibration of AVIRIS was calculated using data from Table 1; and spectral and spatial stray light were measured using the calibrated monochromator and collimator as shown in Figure 3. The total AVIRIS radiometric calibration accuracy was calculated by taking the square root of the sum of the squares of the values of all these factors. In the laboratory environment at the start of the flight season, the achieved accuracy of 7.3% exceeded the requirement of 10% absolute radiometry.

3. COMPARISON OF CALIBRATION OVER TIME

During the course of the 1987 flight season, assessment of AVIRIS performance in flight was conducted by the AVIRIS project and by several investigators selected and funded by NASA. Results of these investigations are reported in Reference 12. We will summarize here the work done by the AVIRIS project on in-flight performance analysis and the post-flight-season laboratory calibration.

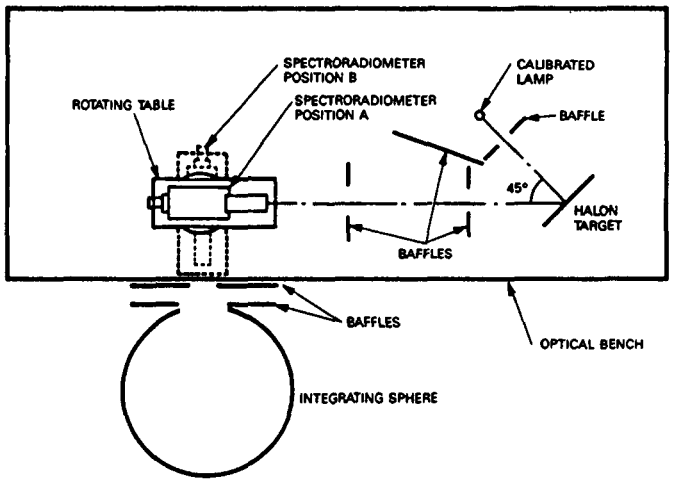

Figure 5. Laboratory setup used in calibrating the AVIRIS spectroradiometer and integrating sphere. All components except the integrating sphere are bolted to an optical bench.[9]

Table 2. AVIRIS 1987 Pre-Flight-Season Radiometric Calibration Error Budget[9]

PARAMETER	MAGNITUDE (%)
INTEGRATING SPHERE CALIBRATION ACCURACY	3.1
AVIRIS THERMALLY INDUCED OUTPUT DRIFT	2.4
AVIRIS VIBRATIONALLY INDUCED OUTPUT DRIFT	
LOW FREQUENCY	2.0
HIGH FREQUENCY	0.7
POLARIZATION SENSITIVITY	5.0
RADIOMETRIC EFFECT OF SPECTRAL CALIBRATION UNCERTAINTY	0.5
SPECTRAL STRAY LIGHT	2.0
SPATIAL STRAY LIGHT	2.0
AVIRIS RADIOMETRIC CALIBRATION ACCURACY	7.3

3.1. Spectral performance over the first flight season

In-flight assessment of the spectral calibration using data acquired at the start of flight operations in June, 1987, confirmed the laboratory calibration summarized above. An example of a full AVIRIS spectrum is shown in Figure 6, which is an average of a 10 by 10 pixel area in the center of Stonewall Playa, Nevada, near the Cuprite Mining District. The playa is a large, uniform surface with only minor spectral structure due to the presence of small amounts of clay, water and Fe^{+3}. The spectral features are thus primarily those of the sun and the atmosphere. The locations and apparent widths of the major atmospheric absorption features were used to assess AVIRIS spectral performance. The spectral wavelength positions of the features were determined using the JPL-developed analysis software SPAM (Spectral Analysis Manager).[13] The first wavelength number is from the AVIRIS data as determined using SPAM; in parentheses are the LOWTRAN 6[14] positions for the features and the atmospheric constituent(s) responsible for the absorption. The figure shows that the AVIRIS and LOWTRAN 6 wavelength positions agree to within 5 nm or better. The widths of the atmospheric absorption features are approximately those that would be expected for an atmospheric spectrum sampled at a 10 nm spectral bandwidth (see following discussion and figures). Thus the in-flight spectral performance of AVIRIS in this early data set agrees well with the laboratory performance.

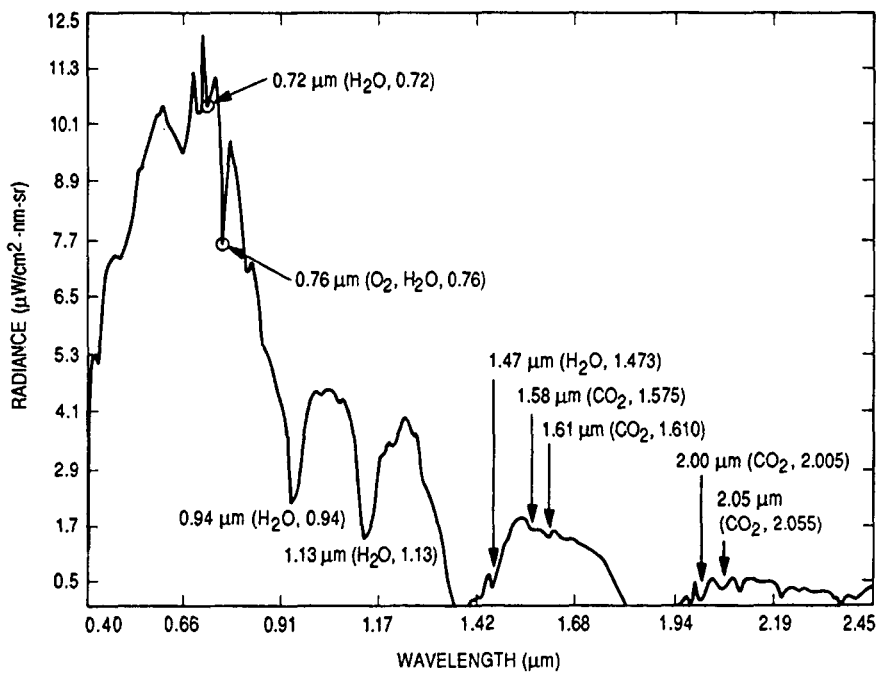

Figure 6. Full spectrum of a 5 by 5 pixel area in the center of Stonewall Playa, Nevada. The data have been radiometrically corrected. The wavelength positions of several atmospheric absorption features are indicated. The first number is the wavelength position derived from the AVIRIS data. In parentheses are the wavelength position of that feature from LOWTRAN 6, and the atmospheric constituent(s) responsible for it (adapted from Reference 26).

During the flight season, the optical fibers carrying the signal from the foreoptics became detached at Spectrometers A and B. A post-flight-season inspection showed that insufficient epoxy had penetrated into the ends of the hypodermic needles holding the fibers at the focus of the spectrometers; mechanical stress from repeated cooling and warming of the instrument during flight operations probably caused the fibers to pull loose and move out of focus. The effects of the defocus are shown in Figure 7, comparing the spectral response functions for each spectrometer measured in the pre- and post-flight-season laboratory calibrations. The FWHM in the post-flight-season calibration for Spectrometers A and B are greater than those of the pre-flight-season calibration, while those of Spectrometers C and D remained unchanged. Their fibers did not detach. Also, the wavelength position of maximum response has shifted by more than 1 nm, which is the measurement threshold in the laboratory, in 3 of the spectrometers. The detached fibers in spectrometers A and B probably explain the wavelength shift in those spectrometers, while warpage of Spectrometer D induced by distortion of the instrument rack probably explains the change in wavelength position of that spectrometer. Table 3 summarizes the laboratory pre- and post-flight-season calibration results for spectral bandwidth and wavelength position.

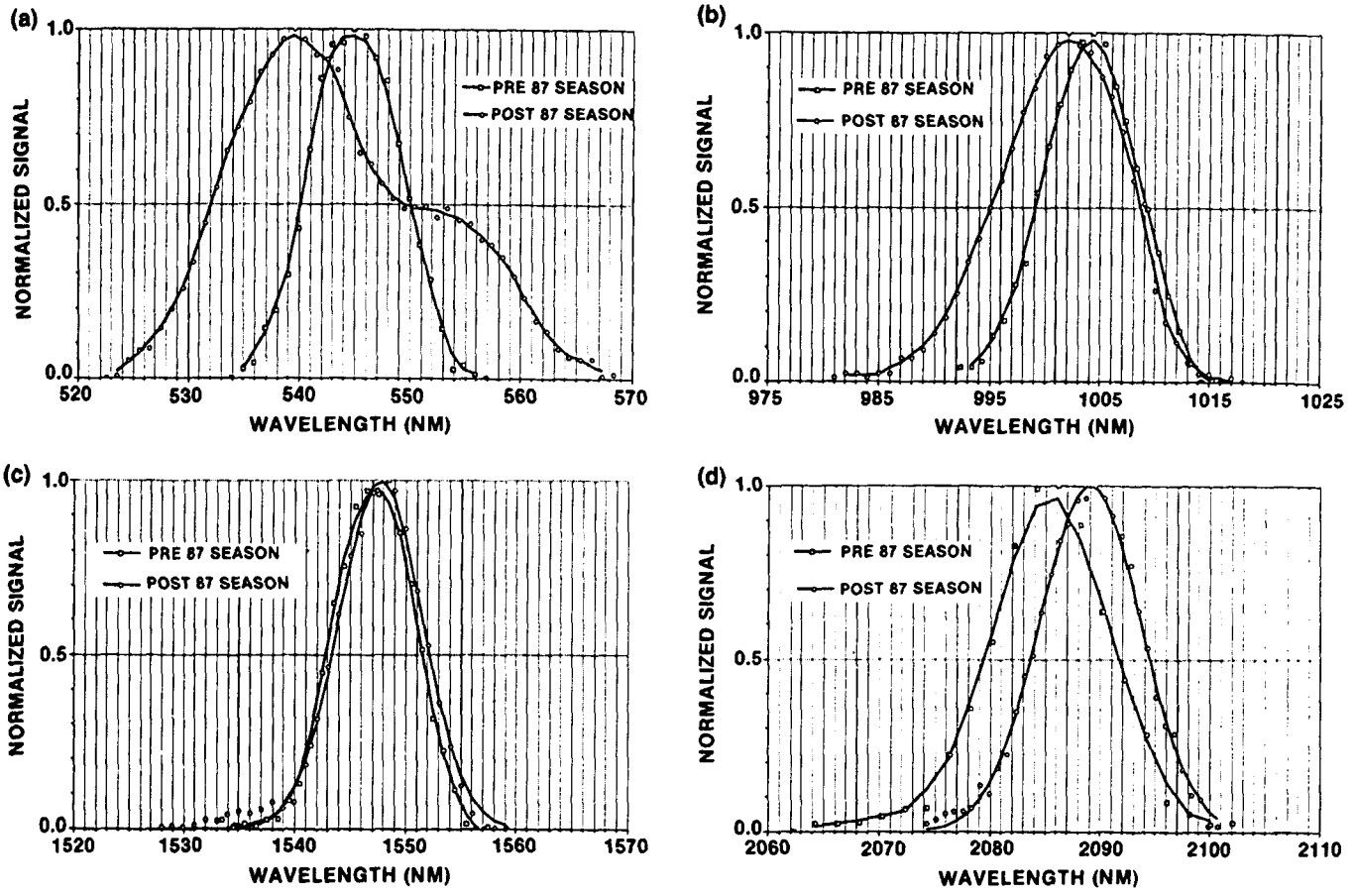

Figure 7. Normalized spectral response functions measured from 4 channels, one from each of the 4 AVIRIS spectrometers, in the 1987 pre- and post-flight-season laboratory calibrations. (a) Spectrometer A, channel 16, (b) Spectrometer B, channel 67, (c) Spectrometer C, channel 128, and (d) Spectrometer D, channel 187.

Table 3. AVIRIS 1987 Pre- and Post-Flight-Season Spectral Response Characteristics

SPECTROMETER (CHANNEL)	FWHM (nm)		λ OF MAXIMUM RESPONSE (nm)	
	PRE-SEASON	POST-SEASON	PRE-SEASON	POST-SEASON
A (16)	10	>17	545	539
B (67)	10	14	1004	1002
C (128)	9	9	1547	1548
D (187)	11	11	2086	2089

A quantitative assessment of the in-flight spectral FWHM and wavelength positions from later in the flight season is shown in Figure 8, comparing atmospheric spectra acquired with Spectrometers B, C and D over Ivanpah Playa, California, on July 30, 1987, with LOWTRAN 6 spectra at full resolution ($\Delta\lambda < 1$ nm) and resampled at the indicated bandwidths. Resampling was done using a Gaussian function with the indicated half-maximum spectral bandwidths. The figure shows that by July 30, 1987, Spectrometer B had become defocussed. A shift in spectral alignment of as much as 10 nm is also suggested. Spectrometers C and D show performance equivalent to that expected for the bandwidths measured in the lab. The spectral alignment of Spectrometer C agrees well with the laboratory calibration

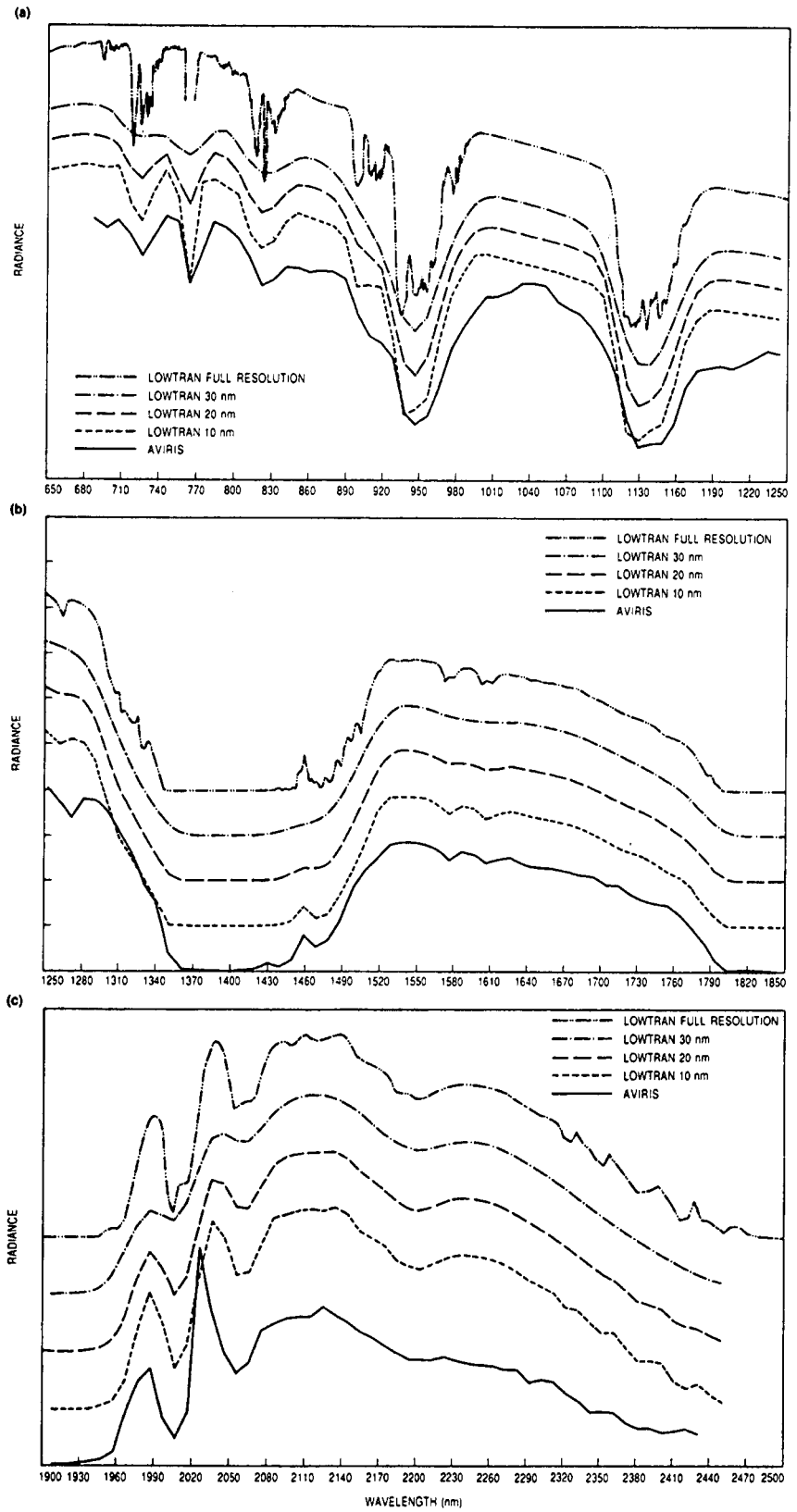

Figure 8. Comparision of AVIRIS atmospheric spectral features over Ivanpah Playa, CA, with LOWTRAN 6 at full resolution, and LOWTRAN 6 resampled at 10, 20, and 30 nm spectral bandwidths. The curves are offset to facilitate comparison between them. (a) Spectrometer B, (b) Spectrometer C, and (c) Spectrometer C.

in these data, while a shift in wavelength of as much as 5 nm in Spectrometer D is suggested. Although the bandwidths and wavelength positions derived from comparison of in-flight data with the LOWTRAN 6 model do not agree precisely with either the pre- or post-flight-season laboratory spectral calibrations, it should be remembered that (1) the instrument response was changing during the flight season, and (2) derivation of spectral performance from assessment of atmospheric absorption features is not as precise as laboratory determinations.

In-flight assessment of the bandwidth and spectral alignment of Spectrometer A is difficult because of the lack of sharp atmospheric absorption features over its region of spectral coverage. An experiment is planned for 1988 using mineral absorption features in this spectral region associated with the carbonatite mine located at Mtn. Pass, California. The Mtn. Pass carbonatite is rich in rare earth elements such as neodydium that contribute several sharp absorption features to the visible portion of its reflectance spectrum.

3.2. Radiometric performance over the first flight season

Detachment of the optical fibers at Spectrometers A and B affected radiometric performance by causing a loss of signal at the detectors. Several other instrument factors also degraded the absolute radiometry of AVIRIS. The thermally-induced warpage to the spectrometer bodies was discussed earlier and found to cause instability in output signal levels of from 2.4% to 7.7% in the laboratory environment.[9] In the much colder aircraft environment, larger instabilities were noted but cannot be quantified due to instabilities in the onboard calibrator in the flight environment. Further, the instrument rack to which the spectrometers are mounted was deformed during the flight season, causing a distortion in the spectrometer bodies that resulted in a loss of optical alignment. This caused an additional loss of signal. Finally, in the post-flight season inspection of AVIRIS, it was discovered that the thermal blocking filter in Spectrometer B had broken during the flight season.

Spectrometer B, which covers the 0.68 to 1.28 μm spectral region, is equipped with two filters[4], a bandpass filter with short- and long-wavelength cutoffs of approximately 0.6 and 2.7 μm, respectively, and a thermal-blocking filter which is opaque to energy beyond 2.0 μm. This dual filter approach was chosen for Spectrometer B because it was not possible to manufacture a bandpass filter with cutoff wavelengths to match its spectral range. Such filters were obtainable for the other 3 spectrometers; hence they each employ a single filter. The short-wavelength cutoff of the bandpass filter assures that no higher order diffracted electromagnetic radiation will be present over the spectral region of interest, while the long-wavelength cutoff of the filter blocks the thermal radiation to which AVIRIS is sensitive. The filters are mounted directly over the detectors on the dewar cold fingers to assure that they are at 77 K to block the thermal background radiation and to minimize their own thermal emissions. The chief source of thermal background radiation in AVIRIS is the spectrometer body itself, which subtends a large portion of the total field of view of the detectors. The spectrometer bodies are thermally controlled to about 300 K and radiate very little energy short of 2.7 μm. Moreover, at a given temperature, the same thermal energy falls on the detector whether it is in the image or dark current readout mode. Hence, subtraction of the detector dark current value which is recorded at the end of each AVIRIS scan will correct for the small thermal background contribution to the signal. However, if the spectrometer body temperature varies between the time of the detector dark current and image acquisition, dark current subtraction does not adequately compensate for the thermal background contribution to the image signal. The original thermal control system for the AVIRIS spectrometers was designed to maintain their temperatures between 296 and 300 K. Our calculations show that a 4 K change in the spectrometer body temperature between the times of the detector readout of the image and dark current, an improbably large change over 1/12 of a second for the massive spectrometer body, would cause an added uncertainty in instrument radiometry of about 2%, if wavelengths as great as 2.7 μm were allowed to fall on the AVIRIS detectors. It was decided to employ an additional blocking filter in spectrometer B to minimize the thermal contributions short of 2.7 μm. A filter cut from a crystal of KH_2PO_4 (KDP) was recommended because of its high transmission over the operating region of spectrometer B and its cutoff wavelength of 2.0 μm. However, it has been subsequently learned that KDP undergoes a solid-state phase transition at about 130 K,[15] and the mechanical stress which results from using it at 77 K in the AVIRIS dewar was the cause of the filter breakage. Some of the cracks in the filter were over the detector array, allowing additional light to fall on the detectors. We also observed during subsequent failure testing of a KDP filter that the phase transition caused a noticeable variation in the transmis sion properties across the filter which varied each of several times the filter was thermally cycled. After the filter cracked, each piece varied in transmission and each piece came to a different state with each successive thermal cycle. We conclude that KDP is not a suitable filter material for use at temperatures below 130 K. We discuss the solution for Spectrometer B in the next section of the paper.

The changes in AVIRIS radiometry resulting from all these effects are shown in Figure 9, where the percentage change between pre- and post-flight-season radiometric calibration multipliers are shown. The multipliers convert DN to radiance through the relation given in Equation 2. If the instrument response were the same at the time of both calibrations, the percent change between the two sets of multipliers would be 0. This is indeed the case for Spectrometer C (spectral channels 97 through 160), which alone of the 4 spectrometers appears not to have suffered degradation during the flight season. For Spectrometer A (channels 1 through 32), the post-flight-season calibration multipliers are from 90% to 180% greater than the pre-flight-season multipliers, indicating a correspondingly lower signal output from the spectrometer for the same radiance input. The Spectrometer B multipliers (channels 33 through 96) are larger for the second calibration by about 100% to 120%, but in addition, there is variation in the percent change in the multipliers across the spectral region of Spectrometer B. This is almost certainly due to solid phase transition-induced variations in transmission and light leakage through the broken KDP filter. Spectrometer D multipliers (channels 161 through 224) are about 20% higher uniformly across its entire spectral region, except for spikes at channels 170, 181, and 210, which are noisy detectors. Although the optical fiber did not detach in this spectrometer, its base was warped by distortion of the instrument rack to which it is mounted, shifting part of the signal off the detectors. A slight shift in wavelength calibration was noted earlier.

On September 14, 1987, a field radiometric calibration experiment was performed at Rogers Dry Lake, California, to assess the validity of the laboratory calibration of AVIRIS.[16] Extinction measurements of the atmosphere were taken by observing the sun from the test site at 5 to 15 minute intervals from sunrise until solar noon, the time of the AVIRIS overflight, using solar radiometers. Total precipitable atmospheric water was measured with a spectral hygrometer. The ratio of direct to diffuse radiation incident at the surface was determined using a hand-held ratioing radiometer (HHRR).[17] On the surface of the dry lake bed, reflectance measurements were made simultaneously with the overflight using the JPL Portable Instantaneous Display and Analysis Spectrometer (PIDAS),[18] and the University of Arizona Barnes Modular Multispectral 8-channel Radiometer (MMR)[19] and Exotech Model 100-AX radiometer.[20] Five different atmospheric

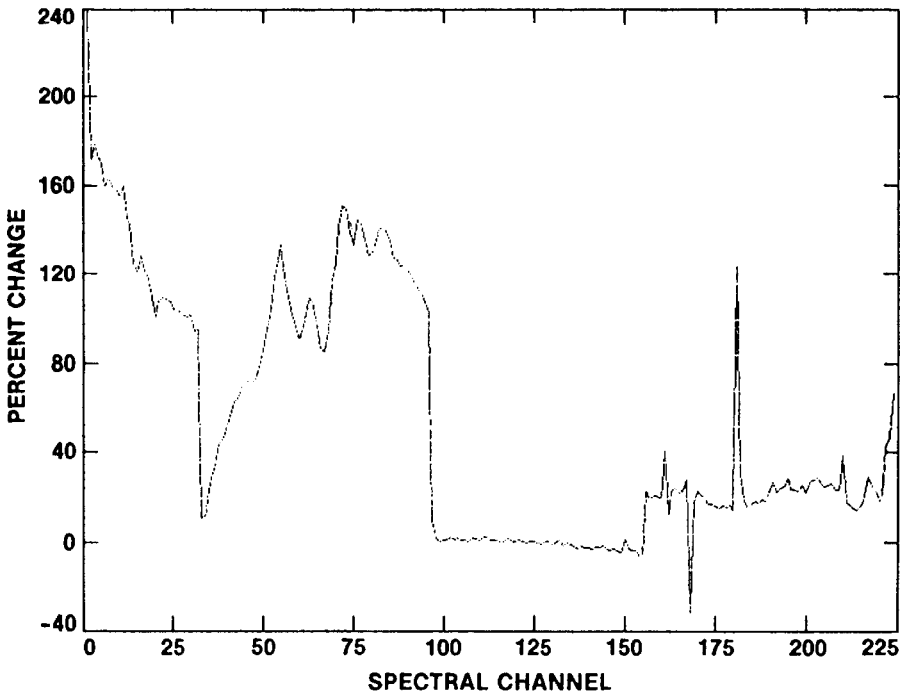

Figure 9. Percent change in the AVIRIS radiometric calibration multipliers, pre- and post-flight-season. Percent change = $(M_{post} - M_{pre})/M_{pre} \times 100$.

models, LOWTRAN 6,[14] LOWTRAN 7,[21] Herman-Browning,[22] Diner-Martonchik,[23] and the 5S code of Tanre et al.[24], were employed. The latter four account for multiple scattering. The measured surface reflectance and atmospheric optical depth were used to particularize the models for flight conditions, and the radiance from the dry lake bed at the instrument was calculated. Good agreement over most of the wavelength region of AVIRIS was found between the 5 models. Figure 10 shows the comparison between the Herman-Browning, Diner-Martonchik, and LOWTRAN 7 generated results, and the AVIRIS-predicted radiance for both the pre- and the post-

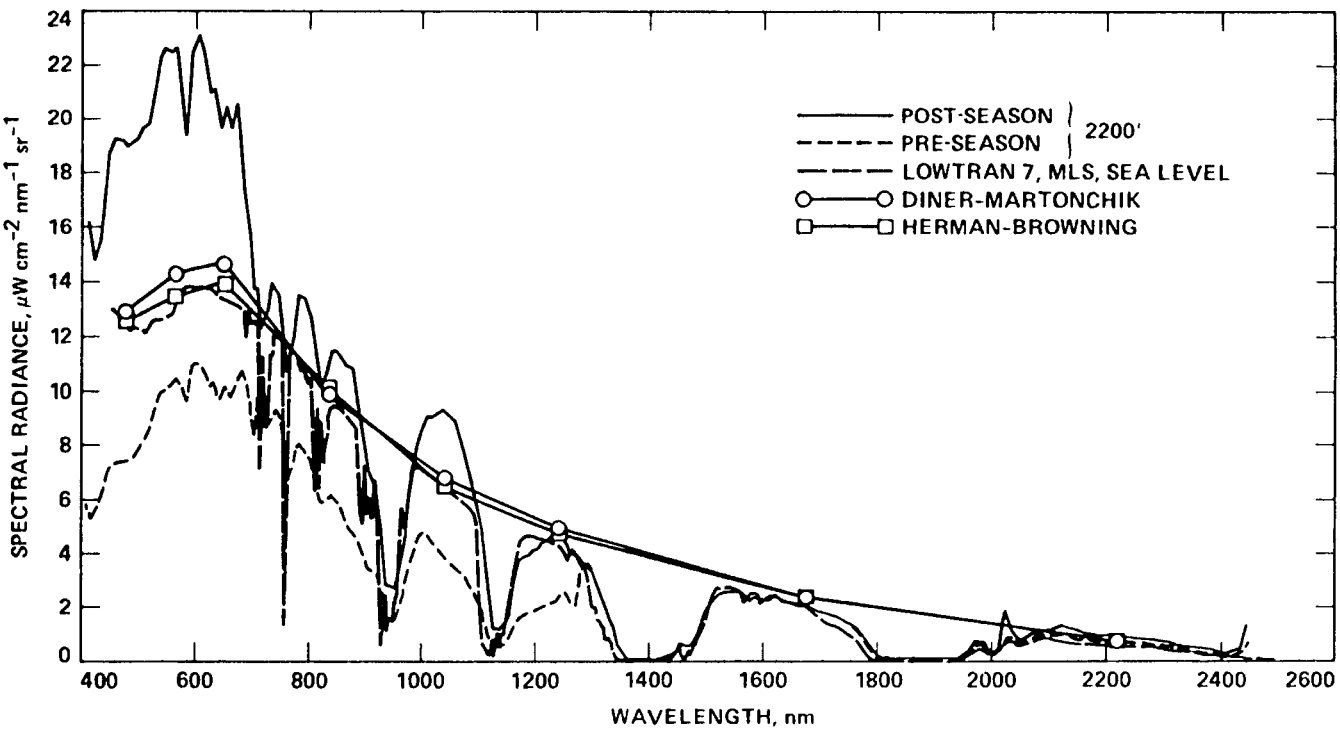

Figure 10. Comparison of three code-generated sets of radiance for Rogers Dry Lake, CA, with the AVIRIS-generated radiance using the pre- and post-flight-season radiometric calibration multipliers.[16]

flight-season calibration multipliers. There is very good agreement between the code-generated and AVIRIS-predicted values over the range of Spectrometer C for both the pre- and post-flight-season calibrations. The discrepancies over the other spectral regions of AVIRIS indicate that instrument response at the time of the overflight was not adequately characterized by either the pre- or post-flight-season calibrations, a reflection of the dynamic nature of instrument performance during the flight season. For a thorough discussion of the field calibration experiment and the results obtained, see Conel et al.[16]

The conclusions from this work are: (1) The validity of the laboratory calibration methodology appears to be confirmed through the agreement achieved over the wavelength range of Spectrometer C between the atmospheric model-generated and the AVIRIS-generated radiance values, but (2) the dynamic nature of the response of the other 3 spectrometers over the course of the 1987 flight season renders the AVIRIS-generated radiance values accurate to no better than 25% to 65% over those spectral regions, depending on the spectrometer and the flight date.

4. IMPROVEMENTS TO AVIRIS AFTER THE FIRST FLIGHT SEASON

All of the known factors that adversely affected AVIRIS spectral and radiometric performance during the first flight season have been resolved as a result of engineering upgrades to the instrument over the past several months. The thermal instability of the spectrometers has been resolved by replacing the thermal control system with a much more sophisticated approach.[25] The system used during the first flight season employed three heater strips on each spectrometer barrel that were commanded to turn on when the spectrometer barrel reached about 296 K and to turn off when the temperature reached 300 K. The new system consists of 24 small heater strips placed evenly over the entire spectrometer body, including the grating and collimator mirror housings and the dewar nose piece. The heaters are on constantly when the temperatures of the spectrometers are at or less than 300 K (room temperature in the calibration laboratory is kept at about 293 K to assure that the heaters are on during spectrometer alignment and focus and during instrument calibration). The output level of the heaters is controlled by a new circuit designed to keep the spectrometer bodies isothermal and at about 300 K plus or minus 0.1 K. The stabilized temperature varies among spectrometers but all are controlled at that temperature to within 0.1 K. Each spectrometer was tested in a cold chamber where it was thermally cycled from room temperature (293 K) to flight temperature (273 K) and back to room temperature. Spectrometer body temperatures were monitored at several places on the structure and a constant optical signal was put into the detectors. Detector output was found to be constant to within 2% over the entire thermal cycle and the spectrometer bodies were found to be isothermal and stable to within the desired tolerance.

To alleviate the effects on the spectrometers of warpage of the instrument rack, the spectrometers have been mounted kinematically on vibration isolators. Spectrometers A, B, and C are on three-point mounts, while Spectrometer D is on a four-point mount because of mechanical packaging constraints. It is expected that this new mounting approach will also provide additional isolation from the instrument and aircraft vibrational environment, and will greatly reduce the heat flow from the spectrometer bodies to the instrument rack, which will aid the effort to keep their temperatures stable.

The tight control on the spectrometer body temperatures achieved with the new heater and controller configuration has made it possible to remove the thermal blocking filter (i.e., the KDP filter) from Spectrometer B. Analysis has shown that if the temperature of the spectrometer body were to vary by as much as 0.1 K between the times of dark current and image acquisition, which is the worst case, the resulting degradation in radiometric precision would be less than 0.1%. Thus the bandpass filter provides adequate blockage of thermal background.

The optical fiber detachment problem has been resolved by using a new epoxy which is less viscous, allowing thorough capillary penetration into the fiber holder. It also has greater holding strength than the epoxy previously used. To verify the improved capillary penetration of the new epoxy, several test fibers were cemented into stainless steel hypodermic needles identical to those used in the AVIRIS spectrometers. After the epoxy had cured, the needles were sectioned in increments of 1 mm. It was found on all the test fibers that the epoxy had penetrated to about 6 mm, which is the desired distance. A new flight fiber package and backup for the foreoptics and the onboard calibrator were made using the new epoxy.

Confirmation of the effectiveness of these changes to the flight hardware is still required. Pre- and post-flight-season laboratory calibrations will be performed on AVIRIS in September and November, 1988, and field radiometric calibration experiments will be conducted in conjunction with the laboratory calibrations. In-flight performance of AVIRIS will also be continuously monitored during the 1988 flight season. Results of our studies of these data will form the basis of a future report on AVIRIS in-flight performance.

5. ACKNOWLEDGEMENTS

The work described in this paper was carried out at the Jet Propulsion Laboratory, California Institute of Technology, under a contract with the National Aeronautics and Space Administration.

6. REFERENCES

1. Vane, G., M. Chrisp, H. Enmark, S. Macenka and J. Solomon, "Airborne Visible/Infrared Imaging Spectrometer: an advanced tool for earth remote sensing," *Proc. 1984 IEEE Int'l. Geoscience and Remote Sensing Symposium*, ESA SP215, 751-757 (1984).

2. Chrisp, M.P., T. Chrien and L. Steimle, "Airborne Visible/Infrared Imaging Spectrometer (AVIRIS) foreoptics, fiber optics and onboard calibrator," *Proc. SPIE Conference on Imaging Spectroscopy II* (San Diego, CA, 20-21 August, 1987), 834, 44-49 (1987).

3. Porter, W.M., and H.T. Enmark, "System overview of the Airborne Visible/Infrared Imaging Spectrometer (AVIRIS)," *Proc. SPIE Conference on Imaging Spectroscopy II* (San Diego, CA, 20-21 August, 1987), 834, 22-31 (1987).

4. Macenka, S.A., and M.P. Chrisp, "Airborne Visible/Infrared Imaging Spectrometer (AVIRIS) spectrometer design and performance," *Proc. SPIE Conference on Imaging Spectroscopy II* (San Diego, CA, 20-21 August, 1987), 834, 32-43 (1987).

5. Bailey, G.C., "Visible and infrared linear detector arrays for the Airborne Visible/Infrared Imaging Spectrometer (AVIRIS)," *Proc. SPIE Conference on Imaging Spectroscopy II* (San Diego, CA, 20-21 August, 1987), 834, 50-54 (1987).

6. Miller, D.C., "Airborne Visible/Infrared Imaging Spectrometer (AVIRIS) scan drive design and performance," *Proc. SPIE Conference on Imaging Spectroscopy II* (San Diego, CA, 20-21 August, 1987), 834, 55-62 (1987).

7. Bunn, J.S., Jr., "Signal chain for the Airborne Visible/Infrared Imaging Spectrometer (AVIRIS)," *Proc. SPIE Conference on Imaging Spectroscopy II* (San Diego, CA, 20-21 August, 1987), 834, 63-68 (1987).

8. Steinkraus, R.E., and R.W. Hickok, "Airborne Visible/Infrared Imaging Spectrometer (AVIRIS) on-board data handling and control," *Proc. SPIE Conference on Imaging Spectroscopy II* (San Diego, CA, 20-21 August, 1987), 834, 69-78 (1987).

9. Vane, G., T.G. Chrien, E.A. Miller and J.H. Reimer, "Spectral and radiometric calibration of the Airborne Visible/Infrared Imaging Spectrometer (AVIRIS)," *Proc. SPIE Conference on Imaging Spectroscopy II* (San Diego, CA, 20-21 August, 1987), 834, 91-106 (1987).

10. Weidner, V.R., and J.J. Hsia, "Reflection properties of pressed polytetrafluoroethylene powder," *J. Opt. Soc. Am.*, 71(7), 856-861 (1981).

11. Bevington, P.R., *Data Reduction and Error Analysis for the Physical Sciences,* McGraw Hill, New York, 336 pp. (1969).

12. Vane, G. (ed.), *Proceedings of the Airborne Visible/Infrared maging Spectrometer (AVIRIS) Performance Evaluation Workshop, JPL Publication,* Jet Propulsion Laboratory, Pasadena, CA, in preparation (1988).

13. Mazer, A.S., M. Martin, M. Lee and J.E. Solomon, "Image processing software for imaging spectrometry data analysis," *Remote Sensing of Environment,* 24(1), 201-210 (1988).

14. Kneizys, F.X., E.P. Shettle, W.O. Gallery, J.H. Chetwynd, Jr., L.W. Abrew, J.E.A. Shelby, S.A. Clough and R.W. Fenn, "Atmospheric transmittance/radiance: Computer code LOWTRAN 6," AFGL-TR-83-0187, AFGL Hanscom AFB, MA, 200 pp. (1983).

15. Cook, W.R., Jr., "Thermal expansion of crystals with KH_2PO_4 structure," *J. Applied Physics,* 38(4), 1637-1642 (1967).

16. Conel, J.E., R.O. Green, R.E. Alley, C.J. Bruegge, V. Carrere, J.S. Margolis, G. Vane, T.G. Chrien, P.N. Slater, S.F. Biggar, P.M. Teillet, R.D. Jackson and M.S. Moran, "In-flight radiometric calibration of the Airborne Visible/Infrared Imaging Spectrometer (AVIRIS)," *Proc. SPIE Conference on Recent Advances in Sensors, Radiometry and Data Processing for Remote Sensing,* (Orlando, FL, 4-8 April, 1988), 924, in press (1988).

17. Whitney, G., M. Abrams and A.F.H. Goetz, "Mineral discrimination using a portable ratio-determining radiometer," *Econ. Geol.,* 78(4), 688-698 (1983).

18. Goetz, A.F.H., "The Portable Instant Display and Analysis Spectrometer (PIDAS)," in *Proc. of the Third Airborne Imaging Spectrometer Data Analysis Workshop* (G. Vane, *ed.*), *JPL Publication 87-30,* Jet Propulsion Laboratory, Pasadena, CA, 8-17 (1987).

19. Robinson, B.F., M.E. Bauer, D.P. Dewitt, L.F. Silva and V.C. Vanderbilt, "Multiband radiometer for field research," *Proc. of the SPIE,* 196, 8-15 (1979).

20. Slater, P.N., S.F. Biggar, R.G. Holm, R.D. Jackson, Y. Mao, M.S. Moran, J.M. Palmer and B. Yuan, "Reflectance- and radiance-based methods for the in-flight absolute calibration of multispectral sensors," *Remote Sensing of Environment,* 22, 11-37 (1987).

21. Kneizys, F.X., E.P. Shettle, G.P. Anderson, L.W. Abrew, J.H. Chetwynd, J.E.A. Shelby, S.A. Clough and W.O. Gallery, "Atmospheric transmittance/radiance: Computer code LOWTRAN 7," in press (1988).

22. Herman, B.M., and S.R. Browning, "The effect of aerosols on the earth-atmosphere albedo," *J. Atmos. Sci.*, 32, 1430-1445 (1975).

23. Diner, D.J., and J.V. Martonchik, "Atmospheric transfer of radiation above an inhomogeneous non-Lambertian reflective ground: I. Theory," *J. Quant. Spectros. Radiat.Transfer.*, 31, 97-125 (1984).

24. Tanre, D., C. Deroo, P. Duhaut, M. Herman, J.J. Morcrette, J. Perbos and P.Y. Dischamps, "Effets atmospheriques en tele-detection-logical de simulation du signal satellitaire dans le spectra solaire," *Proc. Third Int'l. Colloq. on Spectral Signatures of Objects in Remote Sensing,* ESA SP247, 315-319 (1985).

25. Porter, W.M., T.G. Chrien and G. Vane, "Improvements in the Airborne Visible/Infrared Imaging Spectrometer (AVIRIS) since the first flight season," in preparation (1988).

26. Vane, G., "First results from the Airborne Visible/Infrared Imaging Spectrometer (AVIRIS), *Proc. SPIE Conference on Imaging Spectroscopy II* (San Diego, CA, 20-21 August, 1987), 834, 166-174 (1987).